




## RESEARCH ARTICLE

## City size and the spreading of COVID-19 in Brazil

Haroldo V. Ribeiro <sup>1\*</sup>, Andre S. Sunahara<sup>1</sup>, Jack Sutton <sup>2</sup>, Matjaž Perc <sup>3,4,5</sup>, Quentin S. Hanley<sup>2</sup>

**1** Departamento de Física, Universidade Estadual de Maringá, Maringá, Brazil, **2** School of Science and Technology, Nottingham Trent University, Clifton Lane, Nottingham, United Kingdom, **3** Faculty of Natural Sciences and Mathematics, University of Maribor, Maribor, Slovenia, **4** Department of Medical Research, China Medical University Hospital, China Medical University, Taichung, Taiwan, **5** Complexity Science Hub Vienna, Vienna, Austria

\* [hvr@dfi.uem.br](mailto:hvr@dfi.uem.br) OPEN ACCESS

**Citation:** Ribeiro HV, Sunahara AS, Sutton J, Perc M, Hanley QS (2020) City size and the spreading of COVID-19 in Brazil. PLoS ONE 15(9): e0239699. <https://doi.org/10.1371/journal.pone.0239699>

**Editor:** Luo-Luo Jiang, Wenzhou University, CHINA

**Received:** May 29, 2020

**Accepted:** September 11, 2020

**Published:** September 23, 2020

**Copyright:** © 2020 Ribeiro et al. This is an open access article distributed under the terms of the [Creative Commons Attribution License](https://creativecommons.org/licenses/by/4.0/), which permits unrestricted use, distribution, and reproduction in any medium, provided the original author and source are credited.

**Data Availability Statement:** All data supporting the findings of this study are freely available as detailed in the main text.

**Funding:** This research was supported by Coordenação de Aperfeiçoamento de Pessoal de Nível Superior (CAPES) and Conselho Nacional de Desenvolvimento Científico e Tecnológico (CNPq). H.V.R. thanks for the financial support of CNPq (Grant Nos. 407690/2018-2 and 303121/2018-1). M.P. acknowledges financial support of the Slovenian Research Agency (Grant Nos. J4-9302, J1-9112, and P1-0403). The funders had no role in study design, data collection and analysis, decision to publish, or preparation of the manuscript.

## Abstract

The current outbreak of the coronavirus disease 2019 (COVID-19) is an unprecedented example of how fast an infectious disease can spread around the globe (especially in urban areas) and the enormous impact it causes on public health and socio-economic activities. Despite the recent surge of investigations about different aspects of the COVID-19 pandemic, we still know little about the effects of city size on the propagation of this disease in urban areas. Here we investigate how the number of cases and deaths by COVID-19 scale with the population of Brazilian cities. Our results indicate small towns are proportionally more affected by COVID-19 during the initial spread of the disease, such that the cumulative numbers of cases and deaths *per capita* initially decrease with population size. However, during the long-term course of the pandemic, this urban advantage vanishes and large cities start to exhibit higher incidence of cases and deaths, such that every 1% rise in population is associated with a 0.14% increase in the number of fatalities *per capita* after about four months since the first two daily deaths. We argue that these patterns may be related to the existence of proportionally more health infrastructure in the largest cities and a lower proportion of older adults in large urban areas. We also find the initial growth rate of cases and deaths to be higher in large cities; however, these growth rates tend to decrease in large cities and to increase in small ones over time.

## Introduction

Human activities have become increasingly concentrated in urban areas. A direct consequence of this worldwide urbanization process is that more people are living in cities than in rural regions since 2007 [1], and projections indicate that the world urban population could reach more than 90% by the end of this century [2]. Besides being increasingly urbanized, we live in an unprecedentedly connected, and highly mobile world with air passengers exceeding 4 billion in 2018 [3]. On the one hand, a highly connected and highly urbanized society brought us innovation, economic growth, more access to education and healthcare; on the other, it has

**Competing interests:** The authors have declared that no competing interests exist.

also lead to pollution, environmental degradation, privacy concerns, more people living in substandard conditions, and suitable conditions for dissemination of infectious diseases over the globe. In particular, the emergence of infectious disease outbreaks has significantly increased over time, and the majority of these events are caused by pathogens originating in wildlife [4], which in turn has been associated with changes in environmental conditions and land use, agricultural practices, and the rise of large human population settlements [5].

The ongoing outbreak of the novel coronavirus (SARS-CoV-2) seems to fit well the previous context as it was first identified in Wuhan in December 2019, an influential Chinese city exceeding 11 million inhabitants, and apparently originated from the recombination of bat and Malayan pangolin coronaviruses [6]. The coronavirus disease 2019 (COVID-19) initially spread in Mainland China but rapidly caused outbreaks in other countries, making the World Health Organization first declare a “Public Health Emergency of International Concern” in January 2020, and in mid-March, the outbreak was reclassified as a pandemic. As of 16 August 2020, over 21.2 million cases of COVID-19 have been confirmed in almost all countries, and the worldwide death toll exceeds 761 thousand people [7]. The COVID-19 pandemic poses unprecedented health and economic threats to our society, and understanding its spreading patterns may find important factors for mitigating or controlling the outbreak.

Recent works have focused on modeling the initial spreading of COVID-19 [8] or the fatality curves [9], projecting the outbreak peak and hospital utilization [10], understanding the effects of mobility [11], demography [12], travel restrictions [13], behavior change on the virus transmission [14], mitigation strategies [15], non-pharmaceutical interventions [16], network-based strategies for social distancing [17], among many others. Despite the increasing surge of scientific investigations on the subject, little attention has been paid to understanding the effects of city size on spreading patterns of cases and deaths by COVID-19 in urban areas. The idea that size (as measured by population) affects different city indicators has been extensively studied and can be summarized by the urban scaling hypothesis [18–21]. This theory states that urban indicators are non-linearly associated with city population such that socio-economic indicators tend to present increasing returns to scale [18, 22, 23], infrastructure indicators often display economy of scale [18, 19], and quantities related to individual needs usually scale linearly with city population [18, 19].

Urban scaling studies of health-related quantities have shown that the incidence and mortality of diseases are non-linearly related to the city population [24–27]. Despite the existence of several exceptions [27], noninfectious diseases (such as diabetes) are usually less prevalent in large cities, while infectious diseases (such as AIDS) are relatively more common in large urban areas. This different behavior is likely to reflect the fact that people living in large cities tend to have proportionally more contacts and a higher degree of social interactions than those living in small towns [19, 28]. Within this context, the recent work of Stier, Berman, and Bettencourt [29] has indicated that large cities in the United States experienced more pronounced growth rates of COVID-19 cases during the first weeks after the introduction of the disease. Similarly, Cardoso and Gonçalves [30] found that the *per capita* contact rate of COVID-19 increases with the size and density of cities in United States, Brazil and Germany. These findings have serious consequences for the evolution of COVID-19 and suggest that large metropolises may become infection hubs with potentially higher and earlier peaks of infected people. Investigating whether this behavior generalizes to other places and how different quantities such as the number of cases and deaths scale with city size are thus important elements for a better understanding of the spreading of COVID-19 in urban areas.

Here we investigate how population size is associated with cases and deaths by COVID-19 in Brazilian cities. Brazil is the sixth most populous country in the world, with over 211 million people, of which more than 85% live in urban areas. While it is likely that the novel

coronavirus was already circulating in Brazil in early February 2020 [31], the first confirmed case in the country dates back to 26 February 2020, in the city of São Paulo. Between the first case and 12 August 2020, Brazil has confirmed 3,088,670 cases of COVID-19 (second-largest number) spread out over 98.9% of the 5,570 Brazilian cities. This disease caused 102,817 deaths (second-largest number) with 3,892 cities reporting at least one casualty as of 12 August 2020.

## Results

We start by briefly presenting our data set (see [Methods](#) for details). Our investigations rely on the daily reports published by the Health Offices of each of the 27 Brazilian federative units. These daily reports update the number of confirmed cases ( $Y_c$ ) and the number of deaths ( $Y_d$ ) caused by COVID-19 in every Brazilian city from 25 February 2020 (date of the first case in Brazil) to 12 August 2020 (date of our last update). From these data, we create time series of the number of cases  $Y_c(t_c)$  for each city, where  $t_c$  refers to the number of days since the first two daily cases reported in each city. Similarly, we create time series of the number of deaths  $Y_d(t_d)$ , where  $t_d$  refers to the number of days since the first two daily deaths reported in each city. By doing so, we group all cities according to their stage of disease propagation (as measured by  $t_c$  or  $t_d$ ) to investigate the evolution of allometric relationships between total cases or deaths and city population. We have also considered different number of daily cases or deaths as the reference point, and our results are robust against different choices (from one to seven daily cases or daily deaths, see Fig 1-14 in [S1 Appendix](#)).

[Fig 1A](#) shows the relation between cases of COVID-19 and city population on a logarithmic scale ( $\log Y_c$  versus  $\log P$ ) for different numbers of days since the first two daily cases ( $t_c = 15, 58, 101$  and 141 days). The approximately linear behavior on logarithmic scale indicates that

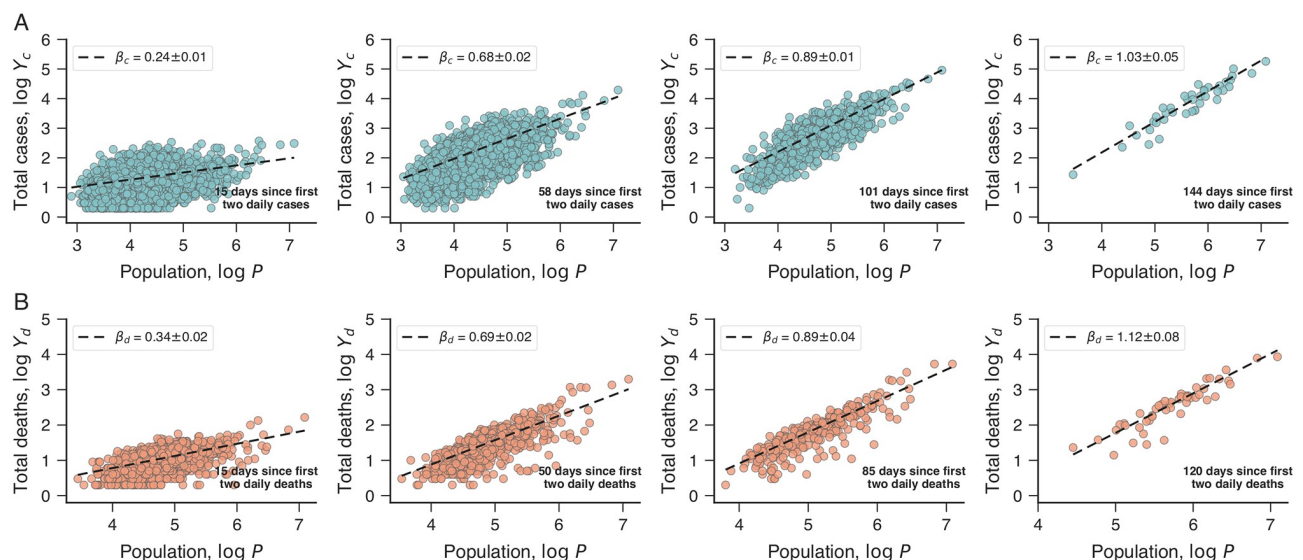


**Fig 1. Urban scaling relations of COVID-19 cases and deaths.** (A) Relationship between the total of confirmed cases of COVID-19 ( $Y_c$ ) and city population ( $P$ ) on logarithmic scale. Panels show scaling relations for the number of cases on a particular day after the first two daily cases reported in each city (four evenly spaced values of  $t_c$  between 15 days and the largest value yielding at least 50 cities, as indicated within panels). (B) Relationship between the total of deaths caused by COVID-19 ( $Y_d$ ) and population ( $P$ ) of Brazilian cities (on logarithmic scale). Panels show scaling relations for the number of deaths on a particular day after the first two daily deaths reported in each city (four evenly spaced values of  $t_d$  between 15 days and the largest value yielding at least 50 cities, as indicated within panels). In all panels, the markers represent cities and the dashed lines are the adjusted scaling relations with best-fitting exponents indicated in each plot ( $\beta_c$  for cases and  $\beta_d$  for deaths).

<https://doi.org/10.1371/journal.pone.0239699.g001>

the number of cases is well described by a power-law function of the city population

$$Y_c \sim P^{\beta_c}, \quad (1)$$

where  $\beta_c$  is the so-called urban scaling exponent [18]. Similarly, Fig 1B shows the association between the number of casualties and the city population on logarithmic scale ( $\log Y_d$  versus  $\log P$ ) for different numbers of days since two daily deaths first reported ( $t_d = 15, 50, 85$  and 120 days). Again, the results indicate that the number of deaths is approximated by a power-function of the city population

$$Y_d \sim P^{\beta_d}, \quad (2)$$

where  $\beta_d$  represents the urban scaling exponent for the number of deaths.

The results of Fig 1 also show the adjusted allometric relationships (dashed lines) and the best fitting scaling exponents  $\beta_c$  and  $\beta_d$  (see Methods for details). These exponents exhibit an increasing trend with time so that  $\beta_c$  and  $\beta_d$  exceed one after some number of days after the first two daily cases or deaths. This dynamic behavior is better visualized in Fig 2, where we depict  $\beta_c$  and  $\beta_d$  as a function of the number of days since the first two daily cases ( $t_c$ ) or deaths ( $t_d$ ). The scaling exponent for the number of cases  $\beta_c$  is sub-linear ( $\beta_c < 1$ ) during the first four months and appears to approach a super-linear plateau ( $\beta_c > 1$ ) as the number of days  $t_c$  further increases. The dynamic behavior of the scaling exponent for deaths  $\beta_d$  is similar to  $\beta_c$ ; however,  $\beta_d$  appears to be approaching a plateau larger than the one observed for  $\beta_c$ .

The evolution of the scaling exponents for cases and deaths indicates that small cities are proportionally more affected by COVID-19 during the first four months. However, this initial apparent advantage of living in large cities vanishes with time, and become a disadvantage after about four months. This is more evident by estimating the number of cases *per capita* from Eq (1), that is,  $Y_c/P \sim P^{\beta_c - 1}$ . Similarly, we can estimate the number of deaths *per capita* from Eq (2), yielding  $Y_d/P \sim P^{\beta_d - 1}$ . Thus, we expect the number of COVID-19 cases or deaths *per capita* to decrease with the city population if  $\beta_c < 1$  and  $\beta_d < 1$ ; conversely, these *per capita* numbers are expected to increase with the city population if  $\beta_c > 1$  and  $\beta_d > 1$ . For instance, because  $\beta_c \approx 0.77$  and  $\beta_d \approx 0.85$  after 75 days since the first two daily cases or deaths, the

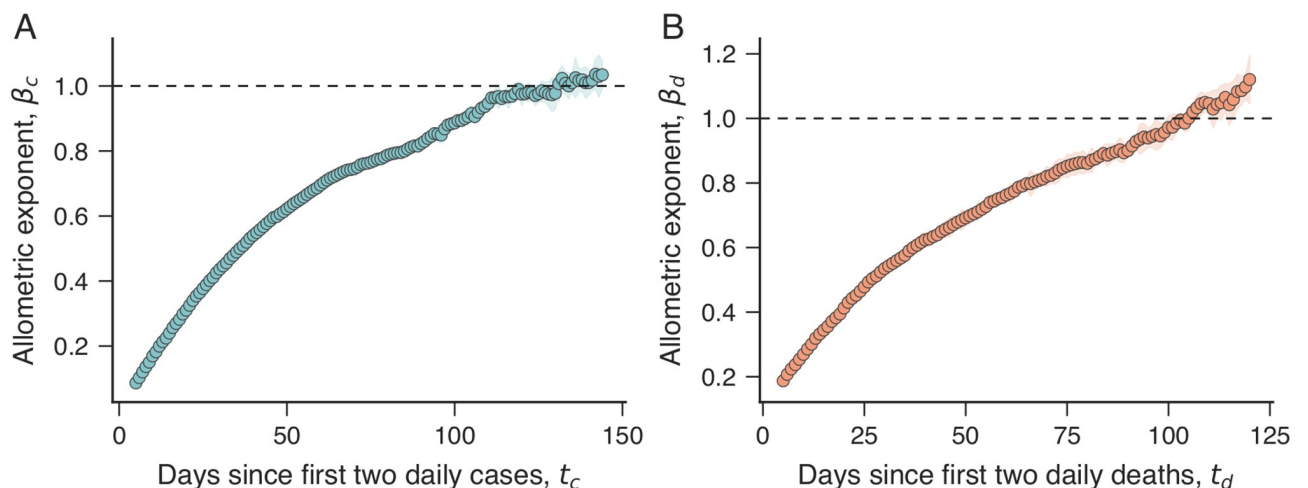


**Fig 2. Time dependence of the scaling exponents for COVID-19 cases and deaths.** (A) Dependence of the exponent  $\beta_c$  on the number of days after the first two daily cases of COVID-19 ( $t_c$ ). (B) Dependence of the exponent  $\beta_d$  on the number of days after the first two daily deaths caused by COVID-19 ( $t_d$ ). The shaded regions in all panels represent bootstrap standard errors, and the horizontal dashed lines indicate the isometric scaling ( $\beta_c = \beta_d = 1$ ). We note that  $\beta_c$  and  $\beta_d$  increase with time and appear to approach asymptotic values larger than one.

<https://doi.org/10.1371/journal.pone.0239699.g002>

number of cases and deaths *per capita* decreases with population as  $Y_c/P \sim P^{-0.23}$  and  $Y_d/P \sim P^{-0.15}$ . At those particular values of  $t_c$  and  $t_d$ , an 1% rise in the population is associated with a  $\approx 0.23\%$  decrease in the incidence of COVID-19 cases and  $\approx 0.15\%$  reduction in the incidence of deaths. In a concrete example for  $t_c = t_d = 75$  days, we expect a metropolis such as São Paulo (with  $\approx 12$  million people) to have  $\approx 54\%$  less cases and  $\approx 39\%$  less deaths *per capita* than a medium-sized city such as Maringá/PR (with  $\approx 420$  thousand people,  $\approx 1/30$  of São Paulo), which in turn is expected to have  $\approx 41\%$  less cases and  $\approx 29\%$  less deaths *per capita* than a small-sized city such as Paranaíba/MS (with  $\approx 42$  thousand people,  $\approx 1/10$  of Maringá).

However, both scaling exponents increase with time, such that this urban advantage vanishes and become a disadvantage during the long course of the pandemic. By considering our latest estimates for the scaling exponents, we find  $\beta_c \approx 1.04$  ( $t_c = 144$  days) and  $\beta_d \approx 1.12$  ( $t_d = 120$  days). Thus, at these particular values of  $t_c$  and  $t_d$ , we expect the number of cases *per capita* to slightly increase with population ( $Y_c/P \sim P^{0.04}$ ) and the number of fatalities *per capita* to increase with population as  $Y_d/P \sim P^{0.12}$ . Thus, for  $\beta_d \approx 1.12$  at  $t_d = 120$  days, we expect a metropolis such as São Paulo ( $\approx 12$  million people) to have  $\approx 50\%$  more deaths *per capita* than Maringá/PR ( $\approx 420$  thousand people), which in turn is expected to have  $\approx 32\%$  more deaths *per capita* than Paranaíba/MS ( $\approx 42$  thousand people). Figs 8-14 in [S1 Appendix](#) show that the scaling relations for number of cases and deaths *per capita* support the previous discussions.

The latest estimates of  $\beta_c$  found for cases of COVID-19 are smaller than those reported for the 2009 H1N1 Pandemic in Brazil ( $\beta_c \approx 1.2$ ) and HIV in Brazil and United States ( $\beta_c \approx 1.4$ ) [27]. Similarly to what we observe for the cases of COVID-19, the allometric exponent for HIV cases in Brazil was initially sub-linear during the 1980s, became super-linear after the 1990s, and started to approach a super-linear plateau after the 2000s [27]. However, the evolution of the allometry for HIV has been much slower than what we have observed for the COVID-19. Another interesting point reported by Rocha, Thorson, and Lambiotte [27] is that the number of H1N1 cases in Brazil started to scale linearly with city population in 2010 (one year after the first outbreak). These authors also argue that this reduction in the scaling exponent possibly reflects a better response for the spread of H1N1 after the pandemic outbreak. If the behavior observed in the 2009 H1N1 Pandemic generalizes (at least in part) for the current COVID-19 pandemic, we would expect a decrease in values of  $\beta_c$  in the future. The latest estimates of  $\beta_d$  for COVID-19 deaths are larger than those reported for diabetes ( $\beta_d \approx 0.8$ ), heart attack ( $\beta_d \approx 1$ ) and cerebrovascular accident ( $\beta_d \approx 1$ ) in Brazil after the 2000s [27]. Conversely, scaling exponents related to disease mortality in Brazil displayed a decreasing trend with time, and values as high as 1.25 were observed for diabetes in 1996 ( $\beta_d \approx 1.22$ ) and heart attack in 1981 ( $\beta_d \approx 1.25$ ) [27]. The convergence of these exponents to linear or sub-linear regimes may reflect the increasing access to medical facilities in urban areas [27].

Based on currently available data (Fig 2), it is hard to confidently assert whether the values of  $\beta_c$  and  $\beta_d$  will remain larger than one during the long-term course of the pandemic. However, the persistence of this behavior indicates large cities are likely to be more affected at the end of the COVID-19 outbreak. Part of this behavior may be due to large cities testing for COVID-19 proportionally more than small ones. Results for the United States indicate that more rural states have lower testing rates and detect disproportionately fewer cases of COVID-19 [32]. As Brazilian cities are likely to suffer from this bias, we would expect a decrease in the scaling exponent  $\beta_c$  after the observed increasing trend depending on the magnitude of this effect (that is, as small cities increase their testing capabilities, their number of cases tend to increase and bend the scaling law downwards).

On the other hand, it is clearer that large cities were proportionately less affected during the initial months (since the first two daily cases or deaths) of the pandemic. We believe there are at least two possible explanations for this behavior. First, it may reflect an “increasing urban

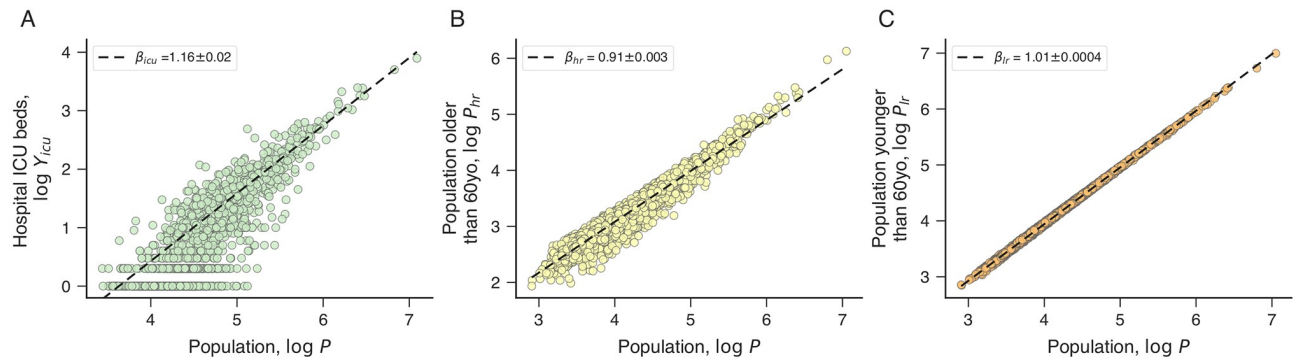


**Fig 3. Urban scaling of ICU beds, high-risk and low-risk populations.** (A) Relationship between the number of ICU beds ( $Y_{icu}$ ) and the city population ( $P$ ) on logarithmic scale. We observe that the number of ICU beds scales super-linearly with city size ( $\beta_{icu} = 1.16 \pm 0.02$ ), indicating an urban advantage for health coverage. (B) Relationship between the high-risk population ( $P_{hr}$ , defined as adults older than 60 years) and the city population ( $P$ ) on logarithmic scale. The high-risk population scales sub-linearly ( $\beta_{hr} = 0.91 \pm 0.003$ ), showing that large cities tend to have smaller fractions of elderly than small cities. (C) Relationship between low-risk population ( $P_{lr}$ , defined as adults younger than 60 years) and the city population ( $P$ ) on logarithmic scale. We note that the low-risk population scales almost linearly ( $\beta_{lr} = 1.01 \pm 0.0004$ ) with city size. The behavior of these three quantities partially explains the initial decrease of number of deaths *per capita* with population ( $\beta_d < 1$  for  $t_d \lesssim 100$  days). See Fig 15 in S1 Appendix for the scaling relations involving *per capita* quantities.

<https://doi.org/10.1371/journal.pone.0239699.g003>

advantage” where the larger the city, the more access to medical facilities and so the chance of receiving more appropriate treatment against the coronavirus disease. A second cause can be associated with age demographic changes with the city population; specifically, a smaller proportion of older adults at high risk for severe illness and death from COVID-19 leads to a reduced number of deaths *per capita*. Another possibility is that the strategies and policy responses of large and small cities to COVID-19 are different, which in turn may lead to different efficiency in containing the pandemic. These responses are highly heterogeneous at the national level [33, 34] as well as among counties in the United States [35]. Among these three possibilities, we did not explore the possible effects of different city strategies against the COVID-19, but in light of the findings for the United States [35], this effect is likely to play an important role in the Brazilian case and may deserve further investigation.

To test for an increasing urban advantage for the treatment of COVID-19 during the initial spread of the disease, we investigate the scaling relation between the number of hospital intensive care unit (ICU) beds and city population. Because critically ill patients frequently require mechanical ventilation [36, 37], the number of ICU beds has proved to be crucial for the treatment of COVID-19. Fig 3A shows the allometric relationship between the number of ICU beds from private and public health systems ( $Y_{icu}$ , as of April 2020) and the population, where a super-linear relationship emerges with scaling exponent  $\beta_{icu} \approx 1.16$ . The super-linear scaling of ICU beds indicates that large Brazilian cities are better structured to deal with critically ill patients, which in turn may partially explain the reduction of deaths *per capita* with the city size during the initial three-four months since the first two daily deaths. It is worth noting that the Brazilian Public Unified Health System (Sistema Único de Saúde—SUS) is decentralized and composed of “health regions”, contiguous groups of cities usually formed by a large city and its neighboring cities [38]. Cities within the same health region may share medical services, which may in turn partially explain the reduction of the structural advantages of large urban areas during the long-term course of the pandemic.

We have also investigated how age demographic distribution changes with city population. Estimates have shown that the case fatality rate of COVID-19 is substantially higher in people aged more than 60 years (0.32% for those younger than 60 years versus 6.5% for those older than 60 years [39]). Thus, the age demographic of cities represents an important factor for the

number of deaths caused by COVID-19. Fig 3B and 3C show how the number of people older ( $P_{hr}$ , the high-risk population) and younger ( $P_{lr}$ , the low-risk population) than 60 years change with the total population ( $P$ ). We note that the high-risk population increases sub-linearly with city size with an exponent  $\beta_{hr} \approx 0.91$ , while the low-risk population scales linearly ( $\beta_{lr} \approx 1$ ) with city size. This result shows that large cities have a lower prevalence of adults older than 60 years, such that a 1% increase in city population is associated with a 0.91% rise in the high-risk population. In a more concrete example, we expect a city with one million people to have proportionally  $\approx 19\%$  fewer adults older than 60 years when compared with a city of 100 thousand inhabitants. Thus, a low prevalence of elderly in large urban areas may also partially explain the initial reduction of the number of deaths *per capita* with the increase of city population.

In addition to addressing the urban scaling of cases and deaths of COVID-19, we have investigated associations between the growth rates of cases and deaths and the city population (Figs 16–22 in S1 Appendix). As mentioned, the work of Stier, Berman, and Bettencourt [29] shows that the initial growth rates of COVID-19 cases in metropolitan areas of the United States scale as a power-law function of the population with an exponent between 0.11 and 0.20. By using our data and as detailed in Methods, we have estimated the growth rates of cases ( $r_c$ ) and deaths ( $r_d$ ) for Brazilian cities. In agreement with the United States case, our results also indicate that COVID-19 cases initially grow faster in large cities (Fig 23 in S1 Appendix), such that  $r_c \sim P^{\beta_{r_c}}$  with  $\beta_{r_c}$  between  $\approx 0.1$  and  $\approx 0.3$  during the first three months ( $t_c \lesssim 90$ , Fig 23 in S1 Appendix). We also found similar behavior for the growth rate in the number of deaths  $r_d$ , where a power-law relation  $r_d \sim P^{\beta_{r_d}}$  is a reasonable description for the empirical data with a scaling exponent  $\beta_{r_d}$  between  $\approx 0.1$  and  $\approx 0.5$  during the first three months ( $t_d \lesssim 90$ , Fig 23 in S1 Appendix).

The growth rate depicts a more instantaneous picture of the COVID-19 spreading process, and its association with size may change during the long-term evolution of the pandemic. These changes may reflect the different actions taken by each city to face the COVID-19 pandemic and other particularities affecting the COVID-19 spreading. For the spreading of COVID-19 in the United States, Heroy [40] has reported that large cities appear to enter in an exponential spreading regime earlier than small ones. To better investigate these possibilities in our data, we have estimated the average relationship between the growth rate of cases ( $r_c$ ) and deaths ( $r_d$ ) and the city rank  $s$  ( $s = 1$  represents the largest city in data,  $s = 2$  the second-largest, and so on) at different periods. Fig 4A shows the results for the growth rates in the number of cases ( $r_c$ ). In agreement with the power-law association between  $r_c$  and the city population (Figs 16–22 in S1 Appendix), we note that lower values of the city rank  $s$  are associated with higher growth rates  $r_c$  in the initial days since the first two daily cases. However, as time goes by, the growth rate of cases starts to decrease in large cities (low-rank values) and to increase in small ones (high-rank values). This result appears to agree with the findings of Heroy [40] in the sense that there is a delay in the emergence of high growth rates of cases between large and small cities. Fig 4B shows the same analysis for growth rate in the number of deaths  $r_d$ . While we also observe a decrease in  $r_d$  for large cities and increase for small ones, the differences in  $r_d$  are less pronounced than in  $r_c$ . These findings also emerge when investigating the scaling exponents associated with the growth rates of cases ( $\beta_{r_c}$ ) and deaths ( $\beta_{r_d}$ ). The results of Fig 23 in S1 Appendix show that these exponents start to decrease around  $t_c \approx t_d \approx 100$  days and become negative in our latest estimates. It is worth remembering that the time  $t_c$  (or  $t_d$ ) is measured in days since the first two daily cases (or first two daily deaths) for each city; thus, the results of Fig 4 do not reflect delays in the emergence of the first case in each city.

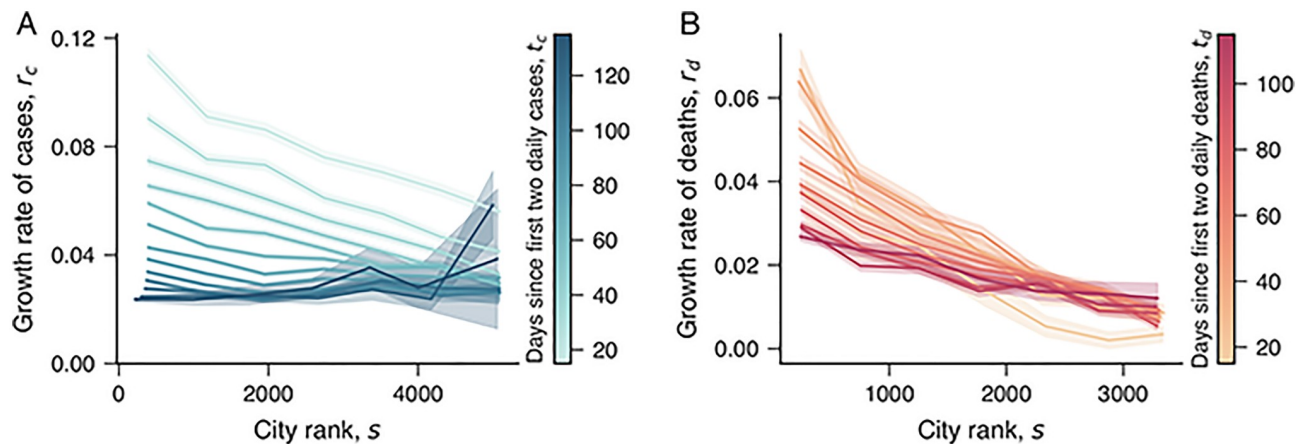


**Fig 4. Association between growth rates and city size.** (A) Relationship between the growth rate of COVID-19 cases ( $r_c$ ) and the city rank ( $s$ ). The different curves show the average values  $r_c$  versus  $s$  for different number of days since the first two daily cases ( $t_c$ , as indicated by the color code). (B) Relationship between the growth rate of deaths by COVID-19 ( $r_d$ ) and the city rank ( $s$ ). The different curves show the average values  $r_d$  versus  $s$  for different number of days since the first two daily deaths ( $t_d$ , as indicated by the color code).

<https://doi.org/10.1371/journal.pone.0239699.g004>

## Discussion

We have studied scaling relations for the number of COVID-19 cases and deaths in Brazilian cities. Similarly to what happens for other diseases, we found the number of cases and deaths to be power-law related to the city population. During the initial three-four months since the first two daily cases or deaths, we found a sub-linear association between cases and deaths by COVID-19, meaning that the *per capita* numbers of cases and deaths tend to decrease with population in this initial stage of the pandemic. We believe this behavior can be partially explained by an “increasing urban advantage” where large cities have proportionally more ICU beds than small ones. In addition, changes in age demography with city size show that large cities have proportionally less elderly people who are at high risk of developing severe illness and dying from COVID-19. This may also partially explain the initial reduction of fatalities *per capita* with the city population. In addition, we have argued that the strategies and policy responses of large and small cities to COVID-19 may also be different and lead to different efficiency in containing the pandemic.

However, we found that this “urban advantage” vanishes in the long-term course of the pandemic, such that the association between cases and deaths by COVID-19 with population becomes super-linear in our latest estimates since the first two daily cases or deaths. Thus, the persistence of this pattern indicates that large cities are expected to be proportionally more affected at the end of the COVID-19 pandemic. This result is in line with the findings for other infectious diseases [25, 27] and probably reflects the existence of a higher degree of interaction between people in large cities [19, 28]. Because social distancing is currently the only available measure to mitigate the impact of COVID-19, our results suggest that large cities may require more severe degrees of social distancing policies.

In agreement with the results for metropolitan areas in the United States [29], we have found that large cities usually display higher growth rates in the number of cases during the initial spread of the COVID-19. However, our results also show that these growth rates tend to decrease in large cities and to increase in small ones in the long-term course of the pandemic. This behavior suggests the existence of a delay in the emergence of high growth rates between large and small cities. Similar behavior was also found in the United States [40], where large cities appear to enter an exponential growth regime earlier than small towns. The existence of



this delay suggests that the initial slow-spreading pace of the COVID-19 in small cities is likely to be a transient behavior.

Together with the recent findings of Stier-Berman-Bettencourt [29] and Heroy [40] for the United States, as well as those of Cardoso and Gonçalves [30] for United States, Brazil and Germany, our results suggest that social distancing policies and other actions against the pandemic should take into account the non-linear effects of city size on the spreading of the COVID-19.

## Methods

### Data

The primary data set used in this work was collected from the `brasil.io` API [41]. This API retrieves information from COVID-19 daily reports published by the Health Offices of each of the 27 Brazilian federations (26 states and one federation district) and makes it freely available. This data set comprises information about the cumulative number of cases and deaths of COVID-19 from 25 February 2020 (date of the first case in Brazil) until 12 August 2020 (date of our last update) for all Brazilian cities reporting at least one case of COVID-19. The `brasil.io` API also provides population data of Brazilian cities, which in turn relies on population estimates for the year 2019 released by the Brazilian Institute of Geography and Statistics (IBGE). There is a total of 5,507 Brazilian cities with at least one reported case of COVID-19 on 12 August 2020, corresponding to 98.9% of the country's total number of cities. In addition, 3,892 cities suffered casualties from this disease, representing 69.9% of the total. To ensure that our estimates rely on at least 50 cities, we consider a suitable upper threshold for the time series length (Fig 24 in [S1 Appendix](#)). The data about age demographics refer to the latest Brazilian census that took place in 2010, while the data about the number of ICU beds are from April 2020. These two data sets are maintained and made freely available by the Department of Informatics of the Brazilian Public Health System (DATASUS) [42].

### Fitting urban scaling laws

Urban scaling [18] usually refers to a power-law association between a city property  $Y$  and the city population  $P$ , and it is expressed by

$$Y = Y_0 P^\beta, \quad (3)$$

where  $Y_0$  is a constant and  $\beta$  is the urban scaling exponent. [Eq \(3\)](#) can be linearized by taking the logarithmic on both sides, that is,

$$\log Y = \log Y_0 + \beta \log P, \quad (4)$$

where  $\log Y$  and  $\log P$  are the dependent and independent variables of the corresponding linear relationship between  $\log Y$  and  $\log P$ . We have estimated the power-law exponents in [Eq \(3\)](#) by using the probabilistic approach of Leitão *et al.* [43]. Specifically, we have found the probabilistic model with lognormal fluctuations and where the fluctuations in  $\log Y$  are independent of  $P$  to be the best description of our data in the majority of scaling laws. Thus, we assume these lognormal fluctuations in all adjusting procedures in order to estimate the values of  $\beta$ . It is worth mentioning that this maximum-likelihood estimate for scaling exponents is analogous to the one obtained via usual least-squares with the log-transformed variables ( $\log Y$  versus  $\log P$ ).

### Logarithmic growth rates of cases and deaths

Let us consider that  $x_t$  ( $t = 1, \dots, n$ ) represents the cumulative number of cases ( $Y_c$ ) or the cumulative number of deaths ( $Y_d$ ) for COVID-19 in a given city at time  $t$  (number of days

since first case  $t_c$  or death  $t_d$ ). The logarithmic growth rate  $r_t$  at time  $t$  is defined as

$$r_t = \log(x_t/x_{t-\tau})/\tau \quad (t = \tau, \tau + 1, \dots, n) \quad (5)$$

where  $\tau$  is a time delay. If we assume the numbers of cases or deaths to initially increase exponentially ( $x_t \sim e^{rt}$ , where  $r$  is the exponential growth rate),  $r_t$  represents an estimate for the growth rate of this initial exponential behavior ( $r$ ). We have estimated  $r_t$  for the number of cases ( $r_c$ ) and deaths ( $r_d$ ) up to values of  $t_c$  and  $t_d$  ensuring a sample size of at least 50 cities for the allometric relations between these growth rates and the city population (Fig 24 in [S1 Appendix](#)). All results in the main text were obtained for  $\tau = 14$  but our discussion is robust for  $\tau$  between 9 and 21 days (Figs 25-38 in [S1 Appendix](#)).

## Supporting information

**S1 Appendix. Supplementary Figs (1-38) supporting the robustness of our findings against different reference points for synchronizing the time series of cases and deaths among cities, different time delays used for estimating the growth rates, and other additional figures.**

(PDF)

## Author Contributions

**Conceptualization:** Haroldo V. Ribeiro, Andre S. Sunahara, Jack Sutton, Matjaž Perc, Quentin S. Hanley.

**Data curation:** Haroldo V. Ribeiro, Andre S. Sunahara, Jack Sutton, Matjaž Perc, Quentin S. Hanley.

**Investigation:** Haroldo V. Ribeiro, Andre S. Sunahara, Jack Sutton, Matjaž Perc, Quentin S. Hanley.

**Visualization:** Haroldo V. Ribeiro, Andre S. Sunahara, Jack Sutton, Matjaž Perc, Quentin S. Hanley.

**Writing – original draft:** Haroldo V. Ribeiro, Andre S. Sunahara, Jack Sutton, Matjaž Perc, Quentin S. Hanley.

**Writing – review & editing:** Haroldo V. Ribeiro, Andre S. Sunahara, Jack Sutton, Matjaž Perc, Quentin S. Hanley.

## References

1. United Nations, World Urbanization Prospects: Urban population (% of total); Available: <http://data.worldbank.org/indicator/SP.URB.TOTL.IN.ZS>.
2. Jiang L, O'Neill BC. Global urbanization projections for the Shared Socioeconomic Pathways. *Global Environ Chang*. 2017; 42:193–199. <https://doi.org/10.1016/j.gloenvcha.2015.03.008>
3. International Civil Aviation Organization, Civil Aviation Statistics of the World and ICAO staff estimates; Available: <https://data.worldbank.org/indicator/IS.AIR.PSGR>.
4. Jones KE, Patel NG, Levy MA, Storeygard A, Balk D, Gittleman JL, et al. Global trends in emerging infectious diseases. *Nature*. 2008; 451(7181):990–993. <https://doi.org/10.1038/nature06536> PMID: 18288193
5. Wolfe ND, Dunavan CP, Diamond J. Origins of major human infectious diseases. *Nature*. 2007; 447(7142):279–283. <https://doi.org/10.1038/nature05775>
6. Xiao K, Zhai J, Feng Y, Zhou N, Zhang X, Zou JJ, et al. Isolation of SARS-CoV-2-related coronavirus from Malayan pangolins. *Nature*. 2020; 583:286–289. <https://doi.org/10.1038/s41586-020-2313-x> PMID: 32380510

7. World Health Organization, Coronavirus disease (COVID-19) Situation Report—209;. Available: [https://www.who.int/docs/default-source/coronaviruse/situation-reports/20200816-covid-19-sitrep-209.pdf?sfvrsn=5dde1ca2\\_2](https://www.who.int/docs/default-source/coronaviruse/situation-reports/20200816-covid-19-sitrep-209.pdf?sfvrsn=5dde1ca2_2).
8. Maier BF, Brockmann D. Effective containment explains subexponential growth in recent confirmed COVID-19 cases in China. *Science*. 2020; 368(6492):742–746. <https://doi.org/10.1126/science.abb4557>
9. Vasconcelos GL, Macêdo AMS, Ospina R, Almeida FAG, Duarte-Filho GC, Souza ICL. Modelling fatality curves of COVID-19 and the effectiveness of intervention strategies. *medRxiv*. 2020. <https://doi.org/10.7717/peerj.9421> PMID: 32612894
10. Moghadas SM, Shoukat A, Fitzpatrick MC, Wells CR, Sah P, Pandey A, et al. Projecting hospital utilization during the COVID-19 outbreaks in the United States. *Proceedings of the National Academy of Sciences*. 2020; 117(16):9122–9126. <https://doi.org/10.1073/pnas.2004064117>
11. Gatto M, Bertuzzo E, Mari L, Miccoli S, Carraro L, Casagrandi R, et al. Spread and dynamics of the COVID-19 epidemic in Italy: Effects of emergency containment measures. *Proceedings of the National Academy of Sciences*. 2020; 117(19):10484–10491. <https://doi.org/10.1073/pnas.2004978117>
12. Dowd JB, Andriano L, Brazel DM, Rotondi V, Block P, Ding X, et al. Demographic science aids in understanding the spread and fatality rates of COVID-19. *Proceedings of the National Academy of Sciences*. 2020; 117(18):9696–9698. <https://doi.org/10.1073/pnas.2004911117>
13. Chinazzi M, Davis JT, Ajelli M, Gioannini C, Litvinova M, Merler S, et al. The effect of travel restrictions on the spread of the 2019 novel coronavirus (COVID-19) outbreak. *Science*. 2020; 368(6489):395–400. PMID: 32144116
14. West R, Michie S, Rubin GJ, Amlôt R. Applying principles of behaviour change to reduce SARS-CoV-2 transmission. *Nature Human Behaviour*. 2020; 4:451–459. <https://doi.org/10.1038/s41562-020-0887-9> PMID: 32377018
15. Walker PG, Whittaker C, Watson OJ, Baguelin M, Winskill P, Hamlet A, et al. The impact of COVID-19 and strategies for mitigation and suppression in low-and middle-income countries. *Science*. 2020; 369:413–422. <https://doi.org/10.1126/science.abc0035> PMID: 32532802
16. Flaxman S, Mishra S, Gandy A, Unwin HJT, Mellan TA, Coupland H, et al. Estimating the effects of non-pharmaceutical interventions on COVID-19 in Europe. *Nature*. 2020; 584:257–261. <https://doi.org/10.1038/s41586-020-2405-7> PMID: 32512579
17. Block P, Hoffman M, Raabe IJ, Dowd JB, Rahal C, Kashyap R, et al. Social network-based distancing strategies to flatten the COVID-19 curve in a post-lockdown world. *Nature Human Behaviour*. 2020; 4:588–596. <https://doi.org/10.1038/s41562-020-0898-6> PMID: 32499576
18. Bettencourt LMA, Lobo J, Helbing D, Kühnert C, West GB. Growth, innovation, scaling, and the pace of life in cities. *Proceedings of the National Academy of Sciences*. 2007; 104(17):7301–7306. <https://doi.org/10.1073/pnas.0610172104>
19. Bettencourt LM. The origins of scaling in cities. *Science*. 2013; 340(6139):1438–1441. <https://doi.org/10.1126/science.1235823> PMID: 23788793
20. Batty M. *The New Science of Cities*. Cambridge, MA: MIT Press; 2013.
21. West GB. *Scale: The Universal Laws of Growth, Innovation, Sustainability, and the Pace of Life in Organisms, Cities, Economies, and Companies*. New York: Penguin; 2017.
22. Youn H, Bettencourt LM, Lobo J, Strumsky D, Samaniego H, West GB. Scaling and universality in urban economic diversification. *Journal of The Royal Society Interface*. 2016; 13(114):20150937. <https://doi.org/10.1098/rsif.2015.0937>
23. Gao J, Zhang YC, Zhou T. Computational socioeconomics. *Physics Reports*. 2019; 817:1–104. <https://doi.org/10.1016/j.physrep.2019.05.002>
24. Acuna-Soto R, Viboud C, Chowell G. Influenza and pneumonia mortality in 66 large cities in the United States in years surrounding the 1918 pandemic. *PLoS One*. 2011; 6(8):e23467. <https://doi.org/10.1371/journal.pone.0023467>
25. Antonio FJ, de Picoli S Jr, Teixeira JJV, dos Santos Mendes R. Growth patterns and scaling laws governing AIDS epidemic in Brazilian cities. *PLoS ONE*. 2014; 9(10):e111015. <https://doi.org/10.1371/journal.pone.0111015>
26. Melo HPM, Moreira AA, Batista É, Makse HA, Andrade JS. Statistical signs of social influence on suicides. *Scientific Reports*. 2014; 4(1):1–6. <https://doi.org/10.1038/srep06239> PMID: 25174706
27. Rocha LE, Thorson AE, Lambiotte R. The non-linear health consequences of living in larger cities. *Journal of Urban Health*. 2015; 92(5):785–799. <https://doi.org/10.1007/s11524-015-9976-x>
28. Schläpfer M, Bettencourt LM, Grauwin S, Raschke M, Claxton R, Smoreda Z, et al. The scaling of human interactions with city size. *Journal of the Royal Society Interface*. 2014; 11(98):20130789. <https://doi.org/10.1098/rsif.2013.0789>

29. Stier AJ, Berman MG, Bettencourt L. COVID-19 attack rate increases with city size. arXiv:200310376. 2020;.
30. Cardoso BHF, Gonçalves S. Urban Scaling of COVID-19 epidemics. arXiv:200507791. 2020;.
31. Delatorre E, Mir D, Graf T, Bello G. Tracking the onset date of the community spread of SARS-CoV-2 in Western Countries. medRxiv. 2020.
32. Souch JM, Cossman JS. A Commentary on Rural-Urban Disparities in COVID-19 Testing Rates per 100,000 and Risk Factors. *The Journal of Rural Health*. 2020. <https://doi.org/10.1111/jrh.12450> PMID: 32282964
33. Hsiang S, Allen D, Annan-Phan S, Bell K, Bolliger I, Chong T, et al. The effect of large-scale anti-contagion policies on the COVID-19 pandemic. *Nature*. 2020; 584(7820):262–267. <https://doi.org/10.1038/s41586-020-2404-8> PMID: 32512578
34. Gao J, Yin Y, Jones BF, Wang D. Quantifying Policy Responses to a Global Emergency: Insights from the COVID-19 Pandemic. arXiv:200613853. 2020;.
35. Brandtner C, Bettencourt L, Stier A, Berman MG. Creatures of the state? Metropolitan counties compensated for state inaction in initial US response to COVID-19 pandemic. Mansueto Institute for Urban Innovation Research Paper. 2020;.
36. Grasselli G, Pesenti A, Cecconi M. Critical care utilization for the COVID-19 outbreak in Lombardy, Italy: Early experience and forecast during an emergency response. *JAMA*. 2020; 323(16):1545–1546. <https://doi.org/10.1001/jama.2020.4031> PMID: 32167538
37. Arabi YM, Murthy S, Webb S. COVID-19: A novel coronavirus and a novel challenge for critical care. *Intensive Care Medicine*. 2020; 46:833–836. <https://doi.org/10.1007/s00134-020-05955-1>
38. Castro MC, Massuda A, Almeida G, Menezes-Filho NA, Andrade MV, de Souza Noronha KVM, et al. Brazil's unified health system: the first 30 years and prospects for the future. *The Lancet*. 2019; 394(10195):345–356. [https://doi.org/10.1016/S0140-6736\(19\)31243-7](https://doi.org/10.1016/S0140-6736(19)31243-7)
39. Verity R, Okell LC, Dorigatti I, Winskill P, Whittaker C, Imai N, et al. Estimates of the severity of coronavirus disease 2019: A model-based analysis. *The Lancet Infectious Diseases*. 2020; 20(6):669–677. [https://doi.org/10.1016/S1473-3099\(20\)30243-7](https://doi.org/10.1016/S1473-3099(20)30243-7) PMID: 32240634
40. Heroy S. Metropolitan-scale COVID-19 outbreaks: How similar are they? arXiv:200401248. 2020; The remote server returned an error: (404) Not Found.
41. Brasil.io—Boletins informativos e casos do coronavírus por município por dia.; Available: <https://brasil.io/dataset/covid19/caso/>.
42. Brazil's Public healthcare System (SUS), Department of Data Processing (DATASUS); Available: <http://datasus.saude.gov.br>.
43. Leitao JC, Miotto JM, Gerlach M, Altmann EG. Is this scaling nonlinear? *Royal Society Open Science*. 2016; 3(7):150649. <https://doi.org/10.1098/rsos.150649>